

1 **The climate reconstruction in Shandong Peninsula, North**  
2 **China, during the last millennia based on stalagmite**  
3 **laminae together with a comparison to  $\delta^{18}\text{O}$**

4 **Qing Wang<sup>1\*</sup>, Houyun Zhou<sup>2\*</sup>, Ke Cheng<sup>1</sup>, Hong Chi<sup>1</sup>, Chuan-Chou Shen<sup>3</sup>,**  
5 **Changshan Wang<sup>1</sup>, Qianqian Ma<sup>1</sup>**

6 [1] {Coast Institute of Ludong University, Yantai 264025, China}

7 [2] {School of Geography, South China Normal University, Guangzhou 510631,  
8 China}

9 [3] {High-precision Mass Spectrometry and Environment Change Lab (HISPEC),  
10 Department of Geosciences, National Taiwan University, Taipei 10617, Taiwan,  
11 ROC}

12 \*Correspondence to: Qing Wang (schingwang@126.com), Houyun Zhou  
13 (hyzhou@gig.ac.cn)

14  
15  
16  
17  
18  
19  
20  
21  
22  
23  
24  
25  
26  
27  
28  
29  
30  
31  
32  
33  
34  
35  
36

## 1 **Abstract**

2 Stalagmite ky1, with a length of 75 mm and the upper part (from top to 42.769  
3 mm depth) consisting of 678 laminae, was collected from Kaiyuan Cave in the  
4 coastal area of Shandong Peninsula, northern China, located in a warm temperate  
5 zone in the East Asia monsoon area. Based on high precision dating with the  
6 U-<sup>230</sup>Th technique and continuous counting of laminae, the 1<sup>st</sup> and 678<sup>th</sup> laminae  
7 have been confirmed to be 1894±20 AD and 1217±20 AD from top to bottom,  
8 respectively. By the measurement of laminae thickness and δ<sup>18</sup>O ratios, we  
9 obtained the time series data of thickness of laminae and δ<sup>18</sup>O ratios from 1217±20  
10 AD to 1894±20 AD, analyzed the climatic-environmental meaning of variations in  
11 the thickness of laminae, which have a good correspondence with the cumulative  
12 departure curve of the drought-waterlog index in the historical period. The results  
13 show that, in the ~678 years from 1217±20 AD to 1894±20 AD, both the thickness  
14 of the laminae and the degree of fluctuation in the thickness of the laminae of  
15 stalagmite ky1 have obvious stages of variation and are completely synchronized  
16 with the contemporaneous intensity of the summer monsoons and precipitation as  
17 time changed. There is a negative correlation between the thickness of the laminae  
18 and the summer monsoon intensity and precipitation. There is a positive correlation  
19 between the degree of fluctuation in the thickness of the laminae and both the  
20 intensity of the summer monsoons and the precipitation. Therefore, for the Kaiyuan  
21 Cave in the coastal area of both the warm temperate zone and the East Asia  
22 monsoon area, the variations in the thickness of the laminae are not only related to  
23 the change in the climatic factors themselves but also related to the degree of  
24 climatic stability. In the coastal area belonging to the warm temperate zone and the  
25 East Asia monsoon area, the climate change between the LIA (Little Ice Age) and  
26 the MWP (Medieval Warm Period), in addition to less precipitation and low  
27 temperatures (a type of dry and cold climate), also shows an obviously decreasing  
28 trend in the degree of climatic stability.

## 29 **Keywords**

30 Little Ice Age, thickness of laminae, degree of climatic stability, Kaiyuan Cave  
31

1 in Shandong Peninsula of CHINA, the coastal area in the warm temperate zone,  
2 East Asia monsoon area

3

#### 4 **1 Introduction**

5 Calcareous speleothems, which have advantages for precisely dating and high  
6 resolution sampling, are becoming one of the best geological record carriers for  
7 major climate changes (Burns et al., 2003; Cheng et al., 2009; Dykoski et al., 2005;  
8 Genty et al., 2003; Fairchild et al., 2006; Wang et al., 2001; Wang et al., 2008; Qin  
9 et al., 1999; Yuan et al., 2004) and high resolution reconstruction of the  
10 paleoclimate and environment (Committee on Surface Temperature  
11 Reconstructions for the Last 2,000 Years and National Research Council, 2006;  
12 Fleitmann et al., 2003; Hou et al., 2003; McDermott et al., 2001; Paulsen et al.,  
13 2003; Tan et al., 2003; Tan, 2007; Wang et al., 2005; Zhang et al., 2008). In addition  
14 to the most widely used carbon (C) and oxygen (O) stable isotopes and trace  
15 elements, laminae and the growth rate of stalagmites could also be used as proxies  
16 for the paleoclimate environment. However, different authors have very different  
17 climate and environment interpretations relative to thickness of laminae based on  
18 different stalagmites from different climatic regions. For instance, the stalagmite  
19 laminae were confirmed as annual laminae in the earliest studies (Baker et al.,  
20 1993), the structure of the laminae reflected the intensity of the ancient rainfall  
21 (Baker et al., 1999), and there was a positive correlation between the growth rate of  
22 stalagmites and precipitation (Brook et al., 1999). However, there was a negative  
23 correlation between the growth rate of stalagmites and precipitation (Proctor et al.,  
24 2000; Proctor et al., 2002), there was a responsive relationship between the growth  
25 rate of the stalagmites and the winter temperature (Frisia et al., 2003), and the  
26 growth rate of the stalagmites was influenced by the vegetation density on the top  
27 of the cave (Baldini et al., 2005). There was a well-understood relationship between  
28 the speleothem growth rate and climate (Baldini, 2010; Mariethoz et al., 2012). The  
29 situation is more complex in humid and semi-humid regions because other factors  
30 such as drip rate, atmospheric P<sub>CO2</sub> in the cave and the seasonality of the climate

1 may also affect speleothem growth rates (Cai et al., 2011; Duan et al., 2012). The  
2 investigation of stalagmite laminae in the middle reach of the Yangtze River  
3 indicates that the thickness of stalagmite laminae may be regarded as a substitute  
4 index for the summer monsoon intensity in East Asia (Liu et al., 2005). There was a  
5 good response relationship between the variations in the thickness of the laminae  
6 and the variations in rainfall (Tan et al., 1997; Ban et al., 2005). There was a  
7 response relationship between the growth rate of the stalagmites and the  
8 temperature in summer; therefore, the thickness of the laminae may be regarded  
9 as a substitute index for East Asia monsoon intensity (Tan et al., 2004). The  $\delta^{18}\text{O}$   
10 record of ZJD-21 indicates that  $\delta^{18}\text{O}$  in the stalagmite was influenced mainly by the  
11 amount of rainfall and/or the summer/winter rainfall ratio, with lower values  
12 corresponding to wetter conditions and/or more summer monsoon rains (Kuo et al.,  
13 2011). The Wanxiang Cave WX42B record indicates that the stalagmite  $\delta^{18}\text{O}$  has  
14 recorded local/regional moisture change (Li et al., 2011). The growth rate and the  
15 observed temperature had a significant positive correlation (Tan et al., 2013).

16 The upper part of ky1 (from the top to a depth of 42.769 mm, 0-42.769 mm)  
17 consists of 678 continuous clearly transmitting annual laminae because the  
18 transmitting laminae of the stalagmite ky1 are very similar to the annual laminae of  
19 Shihua Cave in Beijing and have all of the typical characteristics of the latter  
20 laminae, which consist of so-called northern type laminae (Zhou et al., 2010).  
21 There are clearly very thin opaque laminae between stalagmite laminae, but the  
22 calcite laminae were thick and transmitting between the stalagmite laminae (Tan et  
23 al., 1999; Tan et al., 2002). Because stalagmite ky1, with a very short length, has  
24 no trace of any weathering, the stalagmite may have stopped growing not long ago.  
25 Its deposition time may be the past several centuries or one millennium, which has  
26 recorded the climatic-environmental information of the Shandong Peninsula since  
27 the late MWP (Medieval Warm Period), including the late MWP, the whole LIA (Little  
28 Ice Age) and the early CWP (Current Warm Period) (Lamp, 1965; Lamp, 1972;  
29 Matthews, 2005; Ogilvie and Jónsson, 2001). In this research, on the basis of high  
30 precision dating with the U-<sup>230</sup>Th technique, we have observed and measured the

1 thickness of the laminae and dated all of the laminae in the upper part of stalagmite  
2 ky1, obtained and researched the time series data on thickness of laminae and  
3 compared these data with the time series data for both the oxygen (O) stable  
4 isotope value and the drought-waterlog index, and we discuss the climatic and  
5 environmental evolution of the coastal part of the warm temperate zone as well as  
6 the East Asia monsoon area since the LIA, especially in the transition periods of  
7 MWP/LIA and LIA/CWP.

8

## 9 **2 Geological setting and sample description**

10 Stalagmite ky1 was collected in 2008 AD from Kaiyuan Cave (36°24'32"N,  
11 118°02'05"E) in western Shandong Peninsula, the coastal area of northern China  
12 (Fig. 1, 2). The cave is located in the northwest hilly area of Lushan Mountain in  
13 Zibo City, Shandong Province, with an elevation of 175 m above sea level (a.s.l.)  
14 (Fig. 2). As the largest peninsula in China, the Shandong Peninsula is located  
15 between the Bohai Sea and the Yellow Sea, and in its western region, the  
16 *Cambrian Middle Zhangxia* formation (mainly the oolitic shale, shale in clip to  
17 thin-layer limestone, oolitic limestone, algal clot limestone) and the *Ordovician*  
18 *Badou* formation and *Gezhuang* formation (mainly for the gray-dark gray thick  
19 layer of mud, wafer-thin limestone, dolomitic limestone and marl) are widely  
20 distributed with a thickness of 24-238 m, including the lower section integrated with  
21 the *Gezhuang* Group and the upper section disconformity in contact with the  
22 Carboniferous *Benxi* formation) (Shandong Provincial Bureau of Geology &  
23 Minerals, 1991), which are the main components of the Lushan Mountain, Yishan  
24 Mountain and Mengshan Mountain with the highest elevation (1108 m, 1031 m and  
25 1150 m, respectively). According to field investigation, the landforms of the  
26 carbonate rocks in montanic caves are well developed, there are many cave  
27 outcroppings on the surface, secondary carbonate sedimentary bodies are  
28 developing well with typical morphological characteristics.

29 Kaiyuan Cave developed in the dolomite of the *Ordovician Zhifangzhuang*  
30 formation with a total thickness of the strata of approximately 110 m. The total

1 length of the cave is 1280 m, the overall distribution is a northwest-southeast strike  
2 with twists and turns, and the space width inside the cave is generally 2 to 8 m and  
3 can be up to 30 m. At the top of the cave, the surface of the bedrock is covered by  
4 soil with a general thickness of 50-80 cm, and the thickest soil was more than 1.0 m.  
5 The soil types are calcareous rocky soil and drab soil ([The Soil and Fertilizer  
6 Workstation of Shandong Province, 1994](#)). The area of Kaiyuan Cave is currently  
7 influenced by both summer and winter monsoons with annual precipitation of ~620  
8 mm and an annual mean temperature of ~13°C, and summer monsoons prevail  
9 during July and August, contributing to half of the annual precipitation ([Fig. 3](#)).

10

### 11 **3 Analytical methods and data processing**

#### 12 **3.1 Establishment of a time scale**

13 The stalagmite ky1 is conical in shape and consists of very pure calcite ([Fig. 4](#)).  
14 The polished surface of the stalagmite and observation of the laminae by  
15 microscope show that stalagmite ky1 had no hiatus during the growing process.  
16 The upper part (0-42.769 mm) comprises 678 laminae overlain by continuous  
17 deposits. All laminae were typical transmitting annual laminae. The stalagmite ky1  
18 has  $^{232}\text{Th}$  concentrations ranging from  $704.6\pm 5.1$  ppt to  $1245.2\pm 5.0$  ppt ([Table 1](#)),  
19 which was determined at the High-precision Mass Spectrometry and Environment  
20 Change Laboratory (HISPEC) of the National Taiwan University using high  
21 precision dating with the U- $^{230}\text{Th}$  technique ([Shen et al., 2002](#)).

22 Because the stalagmite ky1 had no hiatus, the upper part (0-42.769 mm)  
23 contains 678 clear and continuous laminae. These continuous and ongoing  
24 laminae have a clear and definite chronology themselves, pointing to  
25 interpretations. Therefore, based on high precision dating with the U- $^{230}\text{Th}$   
26 technique, we used the method of counting annual laminae to decide the  
27 sedimentation time of each of the laminae and the whole stalagmite ky1 layer by  
28 layer and established the time scale of the stalagmite. In the upper part (0-42.769  
29 mm) of stalagmite ky1, we counted along the upward and downward directions

1 according to some laminae that had high precision dating results with the U-<sup>230</sup>Th  
2 technique, confirming times of formation of the 1<sup>st</sup> and 678<sup>th</sup> laminae first and then  
3 ensuring the age of each of the laminae according to their positions.

### 4 5 **3.2 Measurement of the thickness of the laminae**

6 The stalagmite ky1 was first cut along the growth axis, and a slice was  
7 selected from the profile of the stalagmite and then polished. Second, under the  
8 LEIKA DMRX microscope (magnification of 200×, eyepiece of 10×, objective of  
9 20×), we used transmission light to observe characteristics of the laminae along  
10 the growth axis layer by layer. Third, we measured the thickness of 678 laminae  
11 along three different paths layer by layer, calculated the thickness of every one of  
12 the laminae on average according to the three data points for each of the laminae.  
13 Fourth, we dated every one of the laminae layer by layer and determined the time  
14 series data for the thickness of the laminae of the stalagmite. Finally, we  
15 contrasted the time series data and the  $\delta^{18}\text{O}$  ratio data series, analyzed the  
16 paleoclimate environment characteristic of the different stages and discussed the  
17 climatic-environmental meaning of the variations in the thickness of the laminae.

### 18 19 **3.3 $\delta^{18}\text{O}$ isotope test**

20 First, perpendicular to the growth axis and along the position of 9.5 mm and  
21 18.5 mm from the top, we collected four samples equally spaced at 20 mm from  
22 the growth center that were used for the Hendy test. Second, along the direction of  
23 growth, we collected a 4 mm depth×5 mm width×75 mm length stone strip along  
24 growing axis, and scraped 330 samples using medical scalpel from top to bottom  
25 with a sampling density of 7-8 samples/mm (separation distance of 0.1296 mm on  
26 the average). From the 330 samples, we chose 175 samples to measure their  
27  $\delta^{18}\text{O}$  ratios, basically following the principle of an interval test to avoid the mixed  
28 pollution between adjacent samples. Next, we confirmed the sedimentation time  
29 according to their positions and formed the time series data for  $\delta^{18}\text{O}$  ratios. The  
30  $\delta^{18}\text{O}$  ratios were measured using an automated individual carbonate reaction (Kiel)

1 device coupled with a Thermo-Fisher MAT 253 mass spectrometer at the State  
2 Key Laboratory of Palaeobiology and Stratigraphy of the Nanjing Institute of  
3 Geology and Palaeontology, Chinese Academy of Sciences. Each powdered  
4 sample (~0.08 to 0.1 mg of carbonate) was reacted with 103% H<sub>3</sub>PO<sub>4</sub> at 90°C to  
5 liberate sufficient CO<sub>2</sub> for isotopic analysis. The standard used is NBS-19, and  
6 one standard was analyzed with every ten samples. One sample out of ten was  
7 duplicated to check the replication. All isotope ratios are reported in per mil (‰)  
8 deviations relative to the Vienna Peedee Belemnite (VPDB) standard in the  
9 conventional manner. The standard deviation (1σ) for replicate measurements on  
10 NBS-19 is  $<\pm 0.10\text{‰}$ .

11

## 12 **4 Results and discussion**

### 13 **4.1 The thickness of the stalagmite laminae and the results of dating**

14 In the upper part (0-42.769 mm) of stalagmite ky1, the dating result for ages  
15 corrected in **Table 1** show that the three samples in the positions of 6 mm, 15 mm  
16 and 25 mm are dated at  $1761.9\pm 20.3$  AD,  $1696.6\pm 13.6$  AD and  $1556.4\pm 13.6$  AD,  
17 respectively (**Table 1**). Altogether, there are 221 laminae between the positions of 6  
18 mm and 25 mm, and their age intervals are 206 years according to the U-<sup>230</sup>Th  
19 dating results. The difference in age between the laminae determined by counting  
20 and by U-<sup>230</sup>Th dating is only 15 years. However, there are 109 laminae between  
21 the positions of 6 mm and 15 mm, and their age intervals are 65 years according to  
22 the result of the U-<sup>230</sup>Th dating. There are 112 laminae between the positions of 15  
23 mm and 25 mm, and their age intervals are 141 years according to the results of  
24 U-<sup>230</sup>Th dating. If we use the position of 6 mm as a datum for calculation, the ages  
25 of the 1<sup>st</sup> and 678<sup>th</sup> laminae are  $1894\pm 20.3$  AD and  $1217\pm 20.3$  AD, respectively. If  
26 we use the position of 25 mm as a datum for calculation, the ages of the 1<sup>st</sup> and  
27 678<sup>th</sup> laminae are  $1909\pm 13.6$  AD and  $1232\pm 13.6$  AD, respectively. The age  
28 intervals are only 14 years different. Finally, considering the error of the  
29 measurement of the thickness of the laminae accumulating downward layer by  
30 layer, we chose the 133<sup>rd</sup> of the laminae corresponding to the position of 6 mm as a



1 datum to calculate the age of the other laminae in the upper part of stalagmite ky1.  
2 The results show that the deposition times of the 1<sup>st</sup> and 678<sup>th</sup> laminae are  
3  $1894 \pm 20.3$  and  $1217 \pm 20.3$  AD (the dating error is  $\pm 20.3$  years, similar hereafter for  
4 the AD ages in this paper), respectively, the age of the other laminae were  
5 calculated by analogy. Thus, we obtained the time series data for the thickness of  
6 the laminae of stalagmite ky1 (Fig. 5).

7

## 8 **4.2 Characteristics of the shape of the laminae**

9 Stalagmite ky1 obviously developed continuous transmitting laminae (Fig. 4).  
10 Under the microscope, first, the thickness of the laminae was rather changeable.  
11 The maximum thickness was more than  $800 \mu\text{m}$ , and the minimum thickness was  
12 less than  $15 \mu\text{m}$  (Fig. 6a). Because the variations in the thickness of the laminae  
13 may correspond to the climatic environmental changes when the laminae were  
14 growing, the potential value of these transmitting laminae for reconstructing the  
15 paleoclimate environment is illustrated (Genty et al., 1996; Baker et al., 1999; Tan  
16 et al., 2004; Ban et al., 2005; Liu et al., 2005; Zhang et al., 2008; Muangsong et al.,  
17 2014; Liu et al., 2015). Second, most of the boundaries of the laminae are straight,  
18 but some laminae are obviously curved (Fig. 6b). When we analyzed the  
19 climatic-environmental meaning of the thickness of the stalagmite laminae, we  
20 acquired the laminae thickness values of the same laminae in different paths and  
21 calculated their average values along multiple paths to determine the substituted  
22 index information for climatic-environmental change that had statistical  
23 significance. Third, colors in some of the boundaries of the transmitting laminae  
24 were obviously deeper (Fig. 6c). These laminae had a special structure similar to  
25 supra annual laminae. This special structure may indicate that  
26 climatic-environmental changes not only have seasonal changes but also have  
27 multi-interannual changes. Fourth, the light transmission of some transmitting  
28 laminae is obviously different from the light transmission of adjacent laminae: the  
29 color is deeper, and there are dark spots (Fig. 6a, d). Whether these dark laminae  
30 have some mineralogy and geochemistry characteristics different from other

1 transmitting laminae and what their climatic-environmental significance may be,  
2 these dark laminae may need further and special research in the future.

3

#### 4 **4.3 Variations in the thickness of the laminae**

5 The range of variation in the thickness of the 678 laminae of stalagmite ky1  
6 (upper part) were 13.03–872.8  $\mu\text{m}$ . The age determined for the maximum thickness  
7 (872.8  $\mu\text{m}$ ) of the laminae was 1551 AD. The age determined for the minimum  
8 thickness (13.03  $\mu\text{m}$ ) of the laminae was 1245 AD, and the average value for all  
9 laminae was 63.08  $\mu\text{m}$  (Fig. 7a). In the 678 years from 1217 AD to 1894 AD, the  
10 thickness of the laminae from stalagmite ky1 have obvious stages of variation.  
11 Stalagmite ky1 had undergone the transition from low values to high values and  
12 again to low values, and both the thickness of the laminae and the fluctuating  
13 degree of variation in the thickness of the laminae had obvious stages of variation  
14 (Fig. 7a). From 1217 AD to 1471 AD was the low value period of thickness of the  
15 laminae with an average value of 46.08  $\mu\text{m}$ . Then, the period from 1217 AD to 1372  
16 AD was a relatively low fluctuation period. The period from 1372 AD to 1471 AD  
17 was a period of relatively high fluctuation. The two periods above presented the  
18 trend of rising first and then falling. From 1471 AD to 1744 AD, it was a period of  
19 high value-high fluctuation in the thickness of the laminae, with the average value  
20 of 88.8307  $\mu\text{m}$ . This period could be divided into three secondary high value-high  
21 fluctuation periods, 1471 AD-1548 AD, 1548 AD-1637 AD and 1637 AD-1744 AD.  
22 Every period shows the trend of increasing first and then decreasing. The average  
23 values for the thickness of the laminae were 82.2027  $\mu\text{m}$ , 82.5491  $\mu\text{m}$  and 98.8252  
24  $\mu\text{m}$ , successively. From 1744 AD to 1894 AD, there was a period of relatively low  
25 values of the thickness of the laminae, with a group of peak values appearing in  
26 approximately 1776 AD with an average value of 45.1164  $\mu\text{m}$ . The period from  
27 1217 AD to 1372 AD was a period of relatively low fluctuation. The period from  
28 1744 AD to 1831 AD was a period of relatively high fluctuation. The two periods  
29 above present the trend of rising first and then falling. The period from 1831 AD to  
30 1880 AD was a period of relatively high fluctuation, without a trend of obviously

1 rising or falling. The period of rising was short from 1880 AD to 1894 AD.

2

### 3 **4.4 Variations in the $\delta^{18}\text{O}$ ratio**

4 The variation range of  $\delta^{18}\text{O}$  ratios in the 172 samples above was  
5  $-6.247\text{‰}$ – $-8.599\text{‰}$ , with the maximum value ( $-6.247\text{‰}$ ) appearing in 1603 AD  
6 and the minimum value ( $-8.599\text{‰}$ ) appearing in 1460 AD. The value of all of the  
7 samples was  $-7.674\text{‰}$  on average (Fig. 7c). In the 678 years from 1217 AD to  
8 1894 AD,  $\delta^{18}\text{O}$  ratios had obvious stages of variation. The ratios had undergone a  
9 transition from low values to high values and again to low values, and both the  $\delta^{18}\text{O}$   
10 ratios and the degree of fluctuation of  $\delta^{18}\text{O}$  ratios had obvious stages of variation  
11 (Fig. 7c). From 1217 AD to 1480 AD, there was a period of low values of  $\delta^{18}\text{O}$  ratios  
12 with an average value of  $-8.104\text{‰}$ . The period from 1217 AD to 1384 AD was a  
13 period of relatively low fluctuation. This period had a trend of decreasing slowly.  
14 The period from 1384 AD to 1480 AD was a period of relatively high fluctuation, and  
15 this period showed the trend of rising first and then falling. From 1480 AD to 1746  
16 AD was a period of high value-high fluctuation with an average value of  $-7.301\text{‰}$ .  
17 This period could be divided into three secondary high value-high fluctuation  
18 periods: 1480 AD-1542 AD, 1542 AD-1633 AD and 1633 AD-1746 AD. Every  
19 secondary period had the trend of increasing first and then decreasing or  
20 decreasing first and then increasing. The inflection points appeared in the ages of  
21 1498 AD, 1603 AD and 1663 AD, respectively. The average values of the  $\delta^{18}\text{O}$   
22 ratios were  $-7.393\text{‰}$ ,  $-6.953\text{‰}$  and  $-7.513\text{‰}$ , successively. From 1764 AD to  
23 1894 AD was a low value period with an average value of  $-8.199\text{‰}$ . The period  
24 from 1746 AD to 1831 AD was a period of relatively high fluctuation. This period  
25 showed a trend of rising first and then falling. The period from 1831 AD to 1880 AD  
26 was a period of relatively low fluctuation and did not have a trend of obviously rising  
27 or falling. There was a short rising period from 1880 AD to 1894 AD.

28

### 29 **4.5 Drought/waterlog index variations**

30 To show the relationship between the variations in the thickness of the

1 laminae, the  $\delta^{18}\text{O}$  ratios and the changes in climate, we calculated cumulative  
2 departure values for the drought/water log index in the area of Kaiyuan Cave from  
3 1470 AD to 1894 AD. The data source was the *Yearly Charts of Dryness/Wetness*  
4 *in China for the Last 500-year Period*. The charts are compiled by the Chinese  
5 Academy of Meteorological Sciences of the China Meteorological Administration  
6 according to extensive Chinese historical literature and published by the China  
7 Cartographic Publishing House (Chinese Academy of Meteorological Sciences of  
8 the China Meteorological Administration, 1981). In the charts, the degree of  
9 drought/waterlog is represented by the drought/waterlog index that has five values  
10 including 1, 2, 3, 4 and 5, with 1 representing the waterlog and 5 representing  
11 drought, and its distribution is represented through the index isolines. On the basis  
12 of *Yearly Charts of Dryness/Wetness in China for the Last 500-Year Period*, we  
13 acquired the drought/waterlog indices for the area near Kaiyuan Cave according to  
14 its geographical coordinates, and we checked the drought/waterlog indices again  
15 referring to the local chronicles. We drew a cumulative departure curve from 1470  
16 to 1894 AD with a rising trend representing the changes associated with becoming  
17 dryer and a declining trend representing the change associated with becoming  
18 waterlogged (Fig. 7b). Based on the cumulative departure curve, there was a  
19 period of less precipitation in this area from 1480 to 1744 AD. This period starts  
20 with the transition of MWP/LIA and ends with the transition of LIA/CWP. The  
21 primary fluctuations of this period correspond to the curve of the thickness of the  
22 laminae. (Fig. 7b). The high value-high fluctuation period of the thickness of  
23 stalagmite ky1 laminae above occurred under the background of drought and less  
24 precipitation. However, there is a correlation between the  $\delta^{18}\text{O}$  ratios of stalagmite  
25 ky1 and the change in the summer monsoon intensity and precipitation (Cheng et  
26 al., 2009). So, there is a correlation between the summer monsoon  
27 intensity/precipitation and the growth of stalagmites, the weaker summer monsoon  
28 intensity together with less precipitation may be of benefit to the growth of  
29 stalagmites during LIA.

## 1 4.6 Climatic-environmental meanings of variations in the thickness of the 2 laminae

3 Because of the difference in homologous thickness stages of the laminae and  
4  $\delta^{18}\text{O}$  ratios ranging from 2 years to 14 years, in consideration of the error of the  
5 dating technique was  $\pm 20$  years (the time series data from section 4.1) and the  
6 resolution of the  $\delta^{18}\text{O}$  sample was 3.9 years, we could say the two synchronize with  
7 time variation, i.e., the low value period and the high value period of the  $\delta^{18}\text{O}$  ratios  
8 correspond to the low value period and the high value period of the thickness of the  
9 stalagmite laminae. The low fluctuation period and the high fluctuation period for  
10 the  $\delta^{18}\text{O}$  ratios correspond to the low fluctuation period and high fluctuation period  
11 of thickness of stalagmite laminae (Fig. 7a, c). The analysis result for the  $\delta^{18}\text{O}$   
12 variations showed that  $\delta^{18}\text{O}$  ratios for the four samples were  $-7.506\text{‰}$ ,  $-7.753\text{‰}$ ,  
13  $-7.981\text{‰}$  and  $-7.691\text{‰}$  which for the samples that were collected at a 9.5 mm  
14 distance from the top of the stalagmite and the 5, 10, 15 and 20 mm distance from  
15 the axis of growth, respectively. The  $\delta^{18}\text{O}$  ratios for the four samples that were  
16 collected at an 18.5 mm distance from the top of the stalagmite were  $-6.571\text{‰}$ ,  
17  $-6.671\text{‰}$ ,  $-6.540\text{‰}$  and  $-6.542\text{‰}$ . At 5, 10, 15 and 20 mm distances from the  
18 axis of growth, respectively, and the  $\delta^{18}\text{O}$  ratios were similar for the same laminae  
19 (Table 2). Hence, the Hendy Test carried out for ky1 indicates that calcite in ky1  
20 should be deposited under isotopic equilibrium conditions. The possibility of the  
21 dynamic fractionation of the calcite in the sedimentary process is small; therefore,  
22 the stalagmite  $\delta^{18}\text{O}$  mainly reflects the original external climate signal (Hendy,  
23 1971). Therefore, the stalagmite  $\delta^{18}\text{O}$  can be used to collect and reconstruct the  
24 information on climate change (Tan et al., 2009; Kuo et al., 2011; Li et al., 2011; Tan  
25 et al., 2013; Liu et al., 2015).

26 The obvious synchronization relationship between the variations in the  
27 thickness of the laminae and the  $\delta^{18}\text{O}$  ratios variations in stalagmite ky1 shows a  
28 close relationship between the variations in the deposition rate of the stalagmite  
29 and climate change (Fig. 7). Because Kaiyuan Cave is located in a warm temperate  
30 zone influenced by the East Asia monsoon, its rainy season coincides with high

1 temperatures. The precipitation, carried by the summer monsoon from the low  
2 latitude of the Pacific Ocean, concentrates in summer. However, when the winter  
3 monsoon from the interior Asian continent at a high latitude prevails, there is rare  
4 precipitation. In this research, we interpreted the climatic meanings of the  
5 stalagmite ky1  $\delta^{18}\text{O}$  ratios, based on the relationship between the cumulative  
6 departure of the drought/waterlog index and the curves of the  $\delta^{18}\text{O}$  ratios. The  
7 characteristics of contemporary warm temperate weather, also referring to the  
8 assumption of the Asia monsoon intensity by Cheng et al. (2009) and the  
9 precipitation as is assumed by Zhang et al. (2008) about the climatic meanings of  
10 stalagmite  $\delta^{18}\text{O}$  records, with lower  $\delta^{18}\text{O}$  ratios representing a stronger summer  
11 monsoon and higher  $\delta^{18}\text{O}$  ratios representing a weaker summer monsoon, the  $\delta^{18}\text{O}$   
12 ratios are anti-correlative with precipitation (Fig. 7). There was a strong summer  
13 monsoon-more precipitation period from 1217 AD to 1480 AD, a weak summer  
14 monsoon-less precipitation period from 1480 AD to 1746 AD and a strong summer  
15 monsoon-more precipitation period again from 1746 AD to 1894 AD. The degree of  
16 fluctuation of the summer monsoon intensity and precipitation is not the same or  
17 similar in different periods. As a whole, the degree of fluctuation was lower when  
18 the summer monsoon was stronger and the precipitation was more. The degree of  
19 fluctuation was higher when the summer monsoon was weaker and the  
20 precipitation was less. The period from 1217 AD to 1480 AD can be divided into  
21 one low fluctuation period and one high fluctuation period. The period from 1480  
22 AD to 1746 AD can be divided into three high fluctuation periods. The period from  
23 1746 AD to 1894 AD included a high fluctuation period, a low fluctuation period and  
24 a weaker-less fluctuation period, successively.

25 According to the thickness of the laminae and the  $\delta^{18}\text{O}$  record of stalagmite  
26 ky1, the thickness of the laminae and both summer monsoon intensity and  
27 precipitation have a negative correlation. The higher value period of the thickness  
28 of the laminae corresponds to weaker summer monsoon-less precipitation, and the  
29 lower value corresponds to stronger summer monsoon-more precipitation. The  
30 thickness of the laminae and the degree of fluctuation of the summer monsoon

1 intensity-precipitation have a positive correlation. The period of the higher values  
2 for the thickness of the laminae corresponds to a high degree of fluctuation of the  
3 summer monsoon intensity-precipitation, and a lower value corresponds to a low  
4 degree of fluctuation in the summer monsoon-precipitation. Therefore, Kaiyuan  
5 Cave, in the coastal area both of a warm temperate zone and the East  
6 Asia monsoon area, demonstrates that the variations in the thickness of the  
7 laminae are not only relative to the summer monsoon intensity-precipitation but  
8 also relative to their degree of fluctuation because karstic water cycles faster and  
9 residence time is shorter in the fracture of rock. The dissolution was insufficient and  
10 weak; therefore, the deposition rate and the thickness of the laminae from the  
11 stalagmite were low in the period with more precipitation. However, in the period of  
12 less precipitation, the karstic water cycled slower, and the residence time was  
13 longer in the fracture of the rock. The dissolution was sufficient and strong;  
14 therefore, the deposition rate and the thickness of the laminae of the stalagmite  
15 were high. However, karstic water would be reduced or dry up if the period of less  
16 precipitation lasted for a long time. The period of less precipitation is also bad for  
17 water dissolution and growth of the stalagmite laminae. Under the background of  
18 weaker summer monsoons and less precipitation, the degree of fluctuation of the  
19 summer monsoon intensity-precipitation becomes higher, beneficial to increasing  
20 the average value of the thickness of the laminae of the stalagmite, but the degree  
21 of fluctuation also becomes higher. Because of the degree of fluctuation of the  
22 summer monsoon intensity-precipitation reflecting the degree of climatic  
23 stabilization, according to both the thickness of the laminae and the  $\delta^{18}\text{O}$  record of  
24 stalagmite ky1 from the Kaiyuan Cave, the climate change between MWP and LIA  
25 in the coastal area of both a warm temperate zone and the East Asia monsoon  
26 area, in addition to less precipitation and a lower temperature, also shows that the  
27 degree of climatic stability obviously decreased.

28

## 29 **5 Conclusions**

30 The upper part of stalagmite ky1 (0-42.769 mm) clearly consists of 678

1 continuously transmitting annual laminae. The time of deposition ranges from 1217  
2  $\pm 20$  AD to 1894  $\pm 20$  AD; therefore, the laminae contain the climatic-environmental  
3 change information for the late MWP, the whole LIA and the early CWP. The  
4 analysis shows that both the variations in the thickness of the laminae themselves  
5 and the fluctuating degree of variation in the thickness of the laminae of stalagmite  
6 ky1 have obviously staged characteristics from 1217 AD to 1894 AD. Both the  
7 variations in the thickness of the laminae themselves and the fluctuating degree of  
8 variation in the thickness of the laminae of stalagmite ky1 had undergone the  
9 transition from low values to high values and again to low values, synchronized with  
10 the contemporaneous variations in the  $\delta^{18}\text{O}$  ratios and the degree of fluctuation of  
11 the  $\delta^{18}\text{O}$  ratios. According to the comparison among the thicknesses of the laminae,  
12 the drought/waterlog index and the synchronous  $\delta^{18}\text{O}$  ratios of stalagmite ky1, the  
13 thickness of the laminae and the summer monsoon intensity-precipitation have a  
14 negative correlation. The higher value periods of the thickness of the laminae  
15 correspond to weaker summer monsoon-less precipitation, and low value periods  
16 correspond to stronger summer monsoon-more precipitation. The thickness of the  
17 laminae and the degree of fluctuation of the summer monsoon  
18 intensity-precipitation have a positive correlation. The higher value periods of  
19 thickness of the laminae correspond to a high degree of fluctuation of summer  
20 monsoon intensity/precipitation, and the lower value periods correspond to a low  
21 degree of fluctuation in the summer monsoon-precipitation. Therefore, Kaiyuan  
22 Cave, in the coastal area both of a warm temperate zone and the East  
23 Asia monsoon area, with the relationship between the variations in thickness of the  
24 laminae and climate change, in addition to the effects of climate factor variations  
25 such as temperature and precipitation on the thickness of the laminae, also reflects  
26 closely the degree of fluctuation of the summer monsoon intensity and the degree  
27 of climatic stability. On the whole, there was a period of stronger summer  
28 monsoons from 1217 AD to 1470 AD. The climatic stability was high from 1217 AD  
29 to 1370 AD first and was reduced from 1370 AD to 1470 AD. From 1470 AD to 1740  
30 AD, there was a period of weaker summer monsoon-lower degree of stability that



1 could be divided into three secondary periods with a trend of stronger first and then  
2 weaker or weaker first and then stronger divided by 1550 AD and 1640 AD. Since  
3 1640 AD, the summer monsoon has again entered a strong period. The degree of  
4 stability was high from 1740 AD to 1830 AD, and the degree of stability was  
5 reduced from 1830 AD to 1880 AD. The summer monsoon became weaker for a  
6 short time since 1880 AD.

7 The conclusions of this research can enrich the knowledge about the  
8 climatic-environmental meaning of the thickness of the laminae of a stalagmite and  
9 contribute to the comprehension of the specific manifestation of the MWP and LIA  
10 in the coastal area both of a warm temperate zone and the East Asia monsoon  
11 area of northern China, especially the transition time of MWP/LIA and the period  
12 that the LIA lasted and the climatic characteristics of the LIA, and may also deepen  
13 the research into the climate change in the Asian summer monsoon area based on  
14 the secondary carbonate record in the karst cave.

15

## 16 **Acknowledgments**

17 This research was funded by the National Natural Science Foundation of  
18 China (NNSFC, NO.41171158). U-Th dating was finished in the High-precision  
19 Mass Spectrometry and Environment Change Lab (HISPEC) with support of MOST  
20 (104-2119-M-002-003 to C.-C.S.) and the National Taiwan University (105R7625 to  
21 C.-C.S.). The authors thank Professor Jiang Xiuyang (Fujian Normal University) for  
22 his help in sample collection and high precision dating with the U-Th techniques.

23

## 1 **References**

- 2 Baker, A., Smart, P.L., and Edwards, R.L.: Annual growth banding in a cave  
3 stalagmite. *Nature*, 364, 518-520, 1993.
- 4 Baker, A., Proctor, C.J., and Barnes, W.L.: Variations in stalagmite luminescence  
5 laminae structure at Pool's Cave, England, A.D.1910-1996: Calibration of a  
6 palaeo precipitation proxy. *The Holocene*, 9, 683-688, 1999.
- 7 Baldini, J.U.L.: Cave atmosphere controls on stalagmite growth rate and  
8 palaeoclimate records. Geological Society, London, Special Publications, 336,  
9 283-294, 2010.
- 10 Baldini, J.U.L., McDermott, F., Baker, A., Baldini, L.M., Matthey, D.P., and Railsback,  
11 L.B.: Biomass effects on stalagmite growth and isotope ratios: A 20th century  
12 analogue from Wiltshire, England. *Earth and Planetary Science Letters*, 240,  
13 486-494, 2005.
- 14 Ban, F.M., Pan, G.X., and Wang, X.Z.: Timing and possible mechanism of organic  
15 substances formation in stalagmites liminae from Beijing Shihua Cave.  
16 *Quaternary Sciences*, 25,265-268, 2005. (In Chinese with English abstr.)
- 17 Brook, G.A., Rafter, M.A., Railsback, L.B., Sheen, S.W., and Lundberg, J.: A high  
18 resolution proxy record of rainfall and ENSO since AD 1550 from layering in  
19 stalagmites from Anjohibe cave, Madagascar. *The Holocene*, 9, 695-705,  
20 1999.
- 21 Burns, S.J., Fleitmann, D., Matter, A., Kramers, J., and Al-Subbary, A.A.: Indian  
22 Ocean Climate and an Absolute Chronology over Dansgaard/Oeschger Events  
23 9 to 13. *Science*, 301, 1365-1367, 2003.
- 24 Cai, B., Zhu, J., Ban, F., and Tan, M.: Intra-annual variation of the calcite position  
25 rate of drip water in Shihua Cave, Beijing, China and its implications for  
26 palaeoclimatic reconstructions. *Boreas*, 40, 525-535, 2011.
- 27 Cheng, H., Edwards, R.L., Broecker, W.S., Denton, G.H., Kong, X.G., Wang, Y.-J.,  
28 Zhang, R., and Wang, X.F.: Ice age terminations. *Science*, 236, 248-252,  
29 2009.
- 30 Cheng, H., Edwards, R.L., Shen, C.C., Polyak, V.J., Asmerom, Y., Woodhead, J.,

1 Hellstrom, J., Wang, Y.J., Kong, X.G., Spötl, C., Wang, X.F., and Alexander Jr,  
2 E.C.: Improvements in  $^{230}\text{Th}$  dating,  $^{230}\text{Th}$  and  $^{234}\text{U}$  half-life values, and U-Th  
3 isotopic measurements by multi-collector inductively coupled plasma mass  
4 spectrometry. *Earth and Planetary Science Letters* 371-372, 82-91, 2013.

5 Chinese academy of meteorological sciences of China Meteorological  
6 Administration, 1981. Yearly charts of dryness/wetness in China for the last  
7 500-year period. Beijing, China, China Cartographic Publishing House. (In  
8 Chinese)

9 Committee on Surface Temperature Reconstructions for the Last 2,000 Years and  
10 National Research Council: Surface temperature reconstructions for the last  
11 2000 years. National Academies Press, Washington, D.C., 2006.

12 Duan, W., Cai, B., Tan, M., Liu, H., and Zhang, Y.: The growth mechanism of the  
13 aragonitic stalagmite laminae from Yunnan Xianren Cave, SW China revealed  
14 by cave monitoring. *Boreas*, 41, 113-123, 2012.

15 Dykoski, C.A., Edwards, R. L., Cheng, H., Yuan, D.X., Cai, Y.J., Zhang, M.L., Lin,  
16 Y.S., Qing, J.M., An, Z.S., and Revenaugh, J.: A high-resolution,  
17 absolute-dated Holocene and deglacial Asian monsoon record from Dongge  
18 Cave, China. *Earth Planet. Sci. Lett.*, 233, 71-86, 2005.

19 Fairchild, I.J, Smith, C.L., Baker, A., Fuller, L., Spötl, C., Matthey, D., and McDermott,  
20 F.: Modification and preservation of environmental signals in speleothems.  
21 *Earth-Science Reviews*, 75, 105-153, 2006.

22 Fleitmann, D., Burns, S.J., Mudelsee, M., Neff, U., Kramers, J., Mangini, A., and  
23 Matter, A.: Holocene Forcing of the Indian Monsoon Recorded in a Stalagmite  
24 from Southern Oman. *Science*, 300, 1737-1739, 2003.

25 Frisia, S., Borsato, A., Preto, N., and McDermott, F.: Late Holocene annual growth  
26 in three Alpine stalagmites records the influence of solar activity and the North  
27 Atlantic Oscillation on winter climate. *Earth and Planetary Science Letters*, 216,  
28 411-424, 2003.

29 Genty, D., and Quinif, Y.: Annually laminated sequences in the internal structure of  
30 some Belgian stalagmites importance for paleoclimatology. *Journal of*

1 Sedimentary Research, 66, 275-288, 1996.

2 Genty, D., Blamart, D., Ouahdi, R., Gilmour, M., Baker, A., Jouzel, J., and Van-Exter,  
3 S.: Precise dating of Dansgaard-Oeschger climate oscillations in Western  
4 Europe from stalagmite data. *Nature*, 421, 833-837, 2003.

5 Hendy, C.H.: The isotopic geochemistry of speleothems (Part I). The calculation of  
6 the effects of different modes of formation on the isotopic composition of  
7 speleothems and their applicability as palaeoclimatic indicators. *Geochimica et*  
8 *Cosmochimica Acta*, 35, 801-824, 1971.

9 Hiess, J., Condon, D.J., McLean, N., and Noble, S.R.:  $^{238}\text{U}/^{235}\text{U}$  Systematics in  
10 Terrestrial Uranium-Bearing Minerals. *Science*, 30, 1610-1614, 2012.

11 Hou, J.Z., Tan, M., Cheng, H., and Liu, T.S.: Stable isotope records of plant cover  
12 change and monsoon variation in the past 2200 years: evidence from  
13 laminated stalagmites in Beijing, China. *Boreas*, 32, 304-313, 2003.

14 Jaffey, A.H.K., Flynn, K.F., Glendenin, L.E., Bentley, W.C., and Essling, A.M.:  
15 Precision measurement of half-lives and specific activities of  $^{235}\text{U}$  and  $^{238}\text{U}$ .  
16 *Phys. Rev. C*, 4, 1889-1906, 1971.

17 Kuo, T.Z., Liu, Z.Q., Li, H.C., Wan, N.J., Shen, C.C., and Ku, T.L.: Climate and  
18 environmental changes during the past millennium in central western Guizhou,  
19 China as recorded by Stalagmite ZJD-21. *Journal of Asian Earth Sciences*, 40,  
20 1111–1120, 2011.

21 Lamp, H.H.: The early medieval warm epoch and its sequel. *Palaeogeography,*  
22 *Palaeoclimatology, Palaeoecology*, 1, 13-37, 1965.

23 Lamp, H.H.: *Climate: present, past and future*. Methuen, London, 1972.

24 Li, H.C., Lee, Z.H., Wan, N.J., Shen, C.C., Li, T.Y., Yuan, D.X., and Chen, Y.H.: The  
25  $\delta^{18}\text{O}$  and  $\delta^{13}\text{C}$  records in an aragonite stalagmite from Furong Cave,  
26 Chongqing, China: A-2000-year record of monsoonal climate. *Journal of Asian*  
27 *Earth Sciences*, 40, 1121–1130, 2011.

28 Liu, D.B., Wang, Y.J., Cheng, H., Edwards, R.L., and Kong, X.G.: Cyclic changes of  
29 Asian monsoon intensity during the early mid-Holocene from  
30 annually-laminated stalagmites, central China. *Quaternary Science Reviews*,

- 1 121, 1-10, 2015.
- 2 Liu, Y.H., Hu, C.Y., Huang, J.H., Xie, S.C., and Cheng Zhenghong: The research of  
3 layer thickness of the stalagmite from the middle reaches of the Yangtze River  
4 taken as an proxy of the east Asian summer monsoon intensity. Quaternary  
5 Sciences, 25, 228-234, 2005. (In Chinese with English abstr.)
- 6 Matthews, J.A., and Briffa, K.R.: The "Little Ice Age": Re-evaluation of an evolving  
7 concept. Geografiska Annaler: Series A, Physical Geography, 87, 17-36, 2005.
- 8 Mariethoz, G., Kelly, B.F.J., and Baker, A.: Quantifying the value of laminated  
9 stalagmites for paleoclimate reconstructions. Geophysical Research Letters,  
10 39, L05407, DOI: 10.1029/2012GL050986, 2012.
- 11 McDermott, F., Matthey, D.P., and Hawkesworth, C.: Centennial-scale Holocene  
12 climate variability revealed by a high-resolution speleothem  $\delta^{18}\text{O}$  record from  
13 SW Ireland. Science, 294, 1328-1331, 2001.
- 14 Muangsong, C., Cai, B.G., Pumijumnong, N., Hu, C.Y., and Cheng, H.: An annually  
15 laminated stalagmite record of the changes in Thailand monsoon rainfall over  
16 the past 387 years and its relationship to IOD and ENSO. Quaternary  
17 International, 349, 90-97, 2014.
- 18 Ogilvie, A.E.J., and Jónsson, T.: "Little Ice Age" research: A perspective from  
19 Iceland. Climate Change, 48, 9-52, 2001.
- 20 Paulsen, D.E., Li, H.C., and Ku, T.L.: Climate variability in central China over the  
21 last 1270 years revealed by high-resolution stalagmite records. Quat. Sci. Rev.,  
22 22, 691-701, 2003.
- 23 Proctor, C.J., Baker, A., Barnes, W. L., and Gilmour, M. A.: A thousand year  
24 speleothem proxy record of North Atlantic climate from Scotland. Climate  
25 Dynamics, 16, 815-820, 2000.
- 26 Proctor, C.J., Baker, A., and Barnes, W.: A three thousand year record of North  
27 Atlantic climate. Climate Dynamics, 19, 449-454, 2002.
- 28 Qin, X.G., Tan, M., Liu, T.S., Wang, X.F., Li, T.Y., and Lu, J.P.: Spectral analysis of a  
29 1000-year stalagmite lamina-thickness record from Shihua Cavern, Beijing,  
30 China, and its climatic significance. The Holocene, 9, 689-694, 1999.

- 1 Shandong Provincial Bureau of Geology & Mineral, 1991. The Regional Geology  
2 Records. Beijing, China, Geological Publishing House. (In Chinese)
- 3 Shen, C.C., Edwards, R.L., Cheng, H., Dorale, J.A., Thomas, R.B., Moran, S.B.,  
4 Weinstein, S.E., and Edmonds, H.N.: Uranium and thorium isotopic and  
5 concentration measurements by magnetic sector inductively coupled plasma  
6 mass spectrometry. *Chemical Geology*, 185, 165-178, 2002.
- 7 Shen, C.C., Cheng, H., Edwards, R.L., Moran, S.B., Edmonds, H.N., Hoff, J.A.,  
8 Thomas, R.B.: Measurement of attogram quantities of  $^{231}\text{Pa}$  in dissolved and  
9 particulate fractions of seawater by isotope dilution thermal ionization mass  
10 spectroscopy. *Analytical Chemistry*, 75, 1075-1079, 2003.
- 11 Shen, C.C., Wu, C.C., Cheng, H., Edwards, R.L., Hsieh Y.T., Gallet, S., Chang,  
12 C.C., Li, T.Y., Lam, D.D., Kano, A., Hori M., and Spötl, C.: High-precision and  
13 high resolution carbonate  $^{230}\text{Th}$  dating by MC-ICP-MS with SEM protocols.  
14 *Geochimica et Cosmochimica Acta*, 99, 71-86, 2012.
- 15 Tan, L.C., Cai, Y.J., Cheng, H., An, Z.S., and Edwards R.L.: Summer monsoon  
16 precipitation variations in central China over the past 750 years derived from a  
17 high-resolution absolute-dated stalagmite. *Palaeogeography,*  
18 *Palaeoclimatology, Palaeoecology*, 280, 432-439, 2009.
- 19 Tan, L.C., Yi, L., Cai, Y.J., Shen, C.C., Cheng, H., and An, Z.S.: Quantitative  
20 temperature reconstruction based on growth rate of annually-layered  
21 stalagmite: a case study from central China. *Quaternary Science Reviews*,  
22 72, 137-145, 2013.
- 23 Tan, M., Pan, G.X., Wang, X.F., Qin, X.G., Teng, Y.Z., Song, L.H., and Lin Y.S.:  
24 Stalagmites and environment - Preliminary study on the formation of laminated  
25 stalagmites. *Carsologica sinica*, 18, 197-205, 1999. (In Chinese with English  
26 abstract)
- 27 Tan, M., Hou, J.Z., and Cheng, H.: Methodology of quantitatively reconstructing  
28 paleoclimate from annually laminated stalagmite. *Quaternary Sciences*, 22, 209-219,  
29 2002.
- 30 Tan, M.: High resolution climatic records of China and global change. *Quaternary*

1 Science, 24, 455-462, 2004.

2 Tan M., Liu T.S., Hou, J.Z., Qin, X.G., Zhang, H.C., and Li, T.Y.: Cyclic rapid  
3 warming on centennial-scale revealed by a 2650-year stalagmite record of  
4 warm season temperature. *Geophysical Research Letters*, 30, 1617,  
5 doi:10.1029/2003GL017352, 2003.

6 Tan, M.: Climatic differences and similarities between Indian and East Asian  
7 Monsoon regions of China over the last millennium: a perspective based mainly  
8 on stalagmite records. *International Journal of Speleology*, 36, 75-81, 2007.

9 Tan, M., Liu, D.S., Qin, X.G., Zhong, H., Li, T.Y., Zhao, S.S., Li, H.C., Lu, J.B., and  
10 Lu, X.Y.: Preliminary study on the data from microbanding and stable isotopes  
11 of stalagmites of Beijing Shihua Cave. *Carsologica Sinica*, 16, 1-10, 1997. (In  
12 Chinese with English abstr.)

13 The soil and fertilizer workstation of Shandong Province, 1994. Shandong Soil.  
14 Beijing, China, China Agriculture Press. (In Chinese)

15 Wang, Y.J., Cheng, H., Edwards, R.L., An, Z.S., Wu, J.Y., Shen, C.C., and Dorale,  
16 J.A.: A high-resolution absolute-dated late Pleistocene monsoon record from  
17 Hulu Cave, China. *Science*, 294, 2345-2347, 2001.

18 Wang, Y.J., Cheng, H., Edwards, R.L., He, Y.Q., Kong, X.G., An, Z.S., Wu, J.Y.,  
19 Kelly, M.J., Dykoski, C.A., and Li, X.D.: The Holocene Asian Monsoon: Links to  
20 Solar Changes and North Atlantic Climate. *Science*, 308, 854-857, 2005.

21 Wang, Y.J., Cheng, H., Edwards, R.L., Kong, X.G., Shao, X.H., Chen, S.T., Wu, J.Y.,  
22 Jiang, X.Y., Wang, X.F., and An, Z.S.: Millennial- and orbital-scale changes in  
23 the East Asian monsoon over the past 224000 years. *Nature*, 451, 1090-1093,  
24 2008.

25 Yuan, D.X., Cheng, H., Edwards, R.L., Dykoski, C.A., Kelly, M.J., Zhang, M.L., Qing,  
26 J.M., Lin, Y.S., Wang, Y.J., Wu, J.Y., Dorale, J.A., An, Z.S., and Cai, Y.J.: Timing,  
27 Duration, and Transitions of the Last Interglacial Asian Monsoon. *Science*, 304,  
28 575-578, 2004.

29 Zhang, P.Z., Cheng, H., Edwards, R.L., Chen, F.H., Wang, Y.J., Yang, X.L., Liu, J.,  
30 Tan, M., Wang, X.F., Liu, J.H., An, C.L., Dai, Z.B., Zhou, J., Zhang, D.Z., Jia,

1 J.H., Jin, L.Y., and Johnson, K.R.: A test of climate, sun, and culture  
2 relationships from an 1810-Year Chinese cave record. *Science*, 322, 940-942,  
3 2008.

4 Zhou, H.Y., Wang, Q., and Cai, B.G.: Typical northern type speleothem  
5 micro-layers found in stalagmite KY1 collected from Kaiyuan Cave in  
6 Shandong Province, North China. *Quaternary Sciences*, 30, 441-442, 2010. (In  
7 Chinese)

8

9

10

11



Table 1. U-series isotopic results and ages for stalagmite ky1 from Kaiyuan Cave, Shandong peninsula, Northern China.

Sample ID	1	2	3
Dist. from top (mm)	6.0	15.0	25.0
$^{238}\text{U}$ ppb <sup>a</sup>	347.47± 0.63	434.45± 0.92	334.58± 0.61
$^{232}\text{Th}$ ppt	1245.2± 5.0	959.9± 4.9	704.6± 5.1
$\delta^{234}\text{U}_{\text{measured}}$	1457.9± 5.5	1341.2± 5.1	1320.3± 4.6
$[\text{}^{230}\text{Th}/\text{}^{238}\text{U}]$ activity <sup>c</sup>	0.00652± 0.00014	0.00732± 0.00011	0.01021± 0.00013
$[\text{}^{230}\text{Th}/\text{}^{232}\text{Th}]$ ppm <sup>d</sup>	30.0± 0.68	54.63± 0.89	79.9± 1.2
Age uncorrected BP <sup>f</sup>	289.6± 6.5	341.4± 5.4	480.6± 6.3
Age corrected <sup>c,e</sup> BP <sup>f</sup>	251.1± 20.3	316.4± 13.6	456.6± 13.6
Age corrected <sup>c,e</sup> AD	1761.9± 20.3	1696.6± 13.6	1556.4± 13.6
$\delta^{234}\text{U}_{\text{initial corrected}}$ <sup>b</sup>	1458.9± 5.5	1342.4± 5.1	1322.1± 4.6

Chemistry was performed on July. 8, 2013 with the analysis method of Shen et al. (2003), and instrumental analysis on MC-ICP-MS (Shen et al., 2012). Analytical errors are  $2\sigma$  of the mean.

$$^a[\text{}^{238}\text{U}] = [\text{}^{235}\text{U}] \times 137.818 (\pm 0.65\%) \text{ (Hiess et al., 2012); } \delta^{234}\text{U} = ([\text{}^{234}\text{U}/\text{}^{238}\text{U}]_{\text{activity}} - 1) \times 1000.$$

<sup>b</sup> $\delta^{234}\text{U}_{\text{initial corrected}}$  was calculated based on  $^{230}\text{Th}$  age (T), i.e.,  $\delta^{234}\text{U}_{\text{initial}} = \delta^{234}\text{U}_{\text{measured}} \times e^{\lambda^{234}T}$ , and T is the corrected age.

$$^c[\text{}^{230}\text{Th}/\text{}^{238}\text{U}]_{\text{activity}} = 1 - e^{-\lambda^{230}T} + (\delta^{234}\text{U}_{\text{measured}}/1000)[\lambda_{230}/(\lambda_{230} - \lambda_{234})](1 - e^{-(\lambda_{230} - \lambda_{234})T}), \text{ where } T \text{ is the age.}$$

Decay constants are  $9.1705 \times 10^{-6} \text{ yr}^{-1}$  for  $^{230}\text{Th}$ ,  $2.8221 \times 10^{-6} \text{ yr}^{-1}$  for  $^{234}\text{U}$  (Cheng et al., 2013, EPSL), and  $1.55125 \times 10^{-10} \text{ yr}^{-1}$  for  $^{238}\text{U}$  (Jaffey et al., 1971).

<sup>d</sup>The degree of detrital  $^{230}\text{Th}$  contamination is indicated by the  $[\text{}^{230}\text{Th}/\text{}^{232}\text{Th}]$  atomic ratio instead of the activity ratio.

<sup>e</sup>Age corrections for samples were calculated using an estimated atomic  $^{230}\text{Th}/\text{}^{232}\text{Th}$  ratio of  $4 \pm 2$  ppm. Those are the values for a material at secular equilibrium, with the crustal  $^{232}\text{Th}/\text{}^{238}\text{U}$  value of 3.8. The errors are arbitrarily assumed to be 50%.

<sup>f</sup>BP (Before Present), "present" in this table refers to 2013 AD.

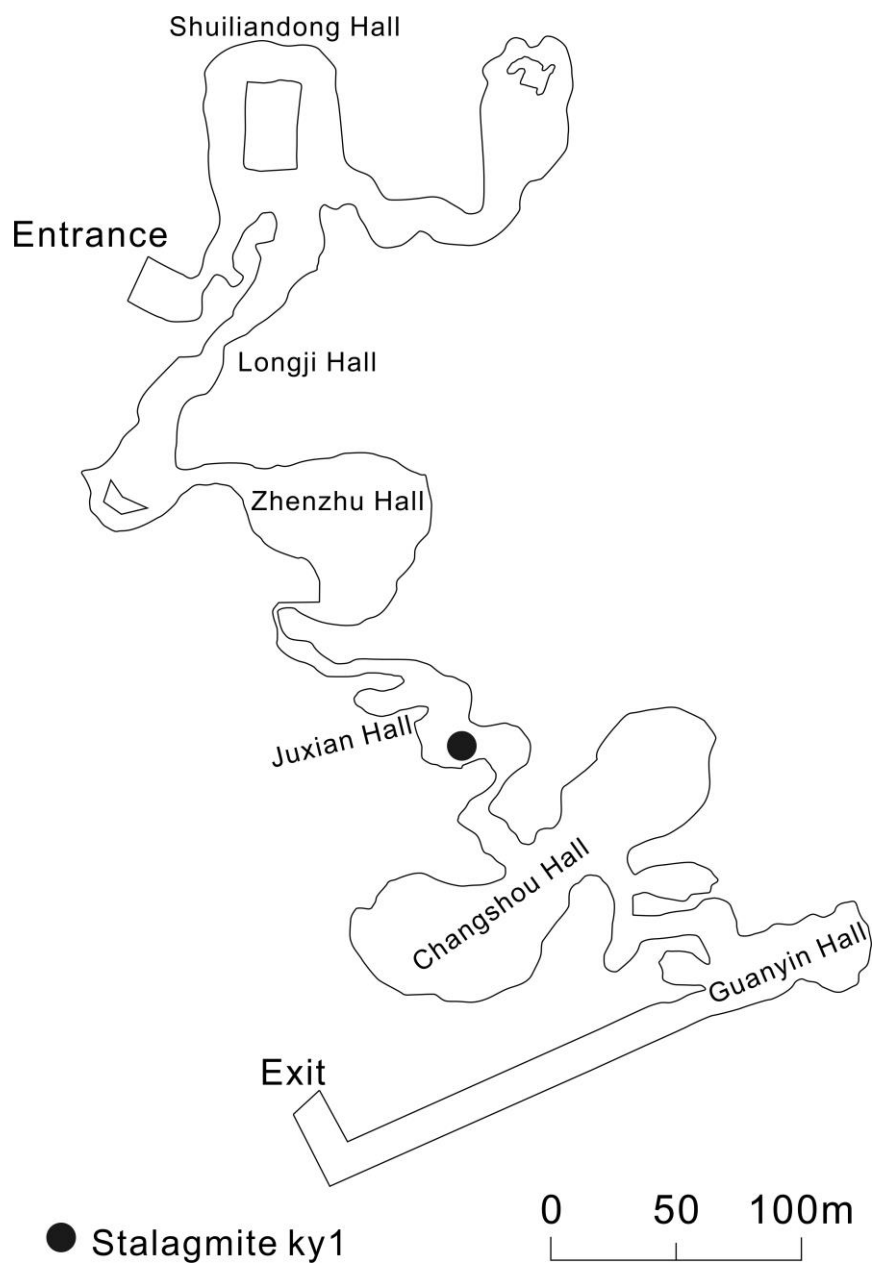
1 Table 2. The results of the Hendy tests conducted along two growth laminae of ky1 at depths of 9.5 mm and  
 2 18.5 mm individually, which indicate that calcite in ky1 was deposited under isotopic equilibrium conditions  
 3 according to the Hendy Test rules (Hendy,1971) .

4

Sample Number	Distance from the Top	Distance from the Center of Growth	$\delta^{18}\text{O}/\text{‰}$
	mm	mm	
KY1-9/10-5		5.0	-7.506
KY1-9/10-10		10.0	-7.753
	9.5		
KY1-9/10-15		15.0	-7.981
KY1-9/10-20		20.0	-7.691
KY1-18/19-5		5.0	-6.571
KY1-18/19-10		10.0	-6.671
	18.5		
KY1-18/19-15		15.0	-6.540
KY1-18/19-20		20.0	-6.542

5

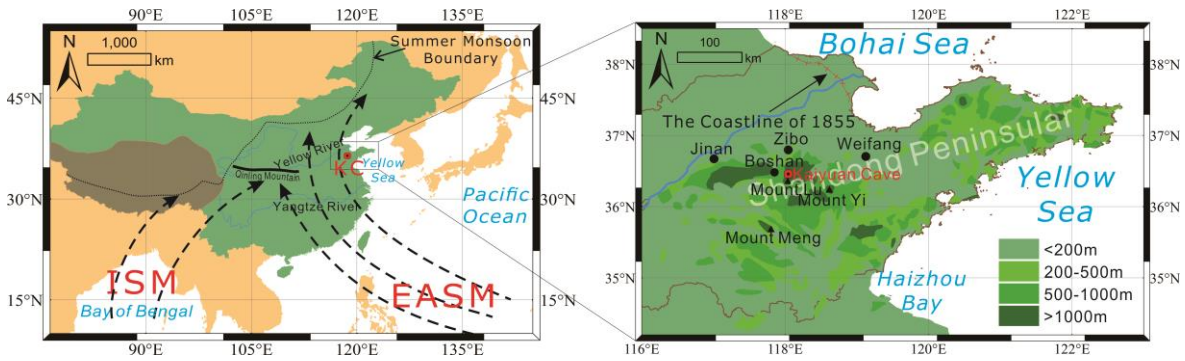
6



1  
2  
3  
4  
5  
6

Fig. 1. The map of Kaiyuan Cave. The black point is the location where we collected the sample in the Cave. The cave has an entrance and an exit, and consists of six small malls.

1



2

3

4 Fig. 2. Location of Kaiyuan Cave and Shandong Peninsula in monsoonal China.

5 KC: Kaiyuan Cave (36°24'32"N, 118°02'05"E). ISM: India Summer Monsoon;

6 EASM: East Asia Summer Monsoon. The dashed black thin line indicates the

7 northwestern boundary of the Asian summer monsoon. The dashed black lines with

8 arrows indicate the routes of the summer monsoon. The dashed black lines with

9 arrows on the left indicate the routes of the summer monsoon. The brown area is

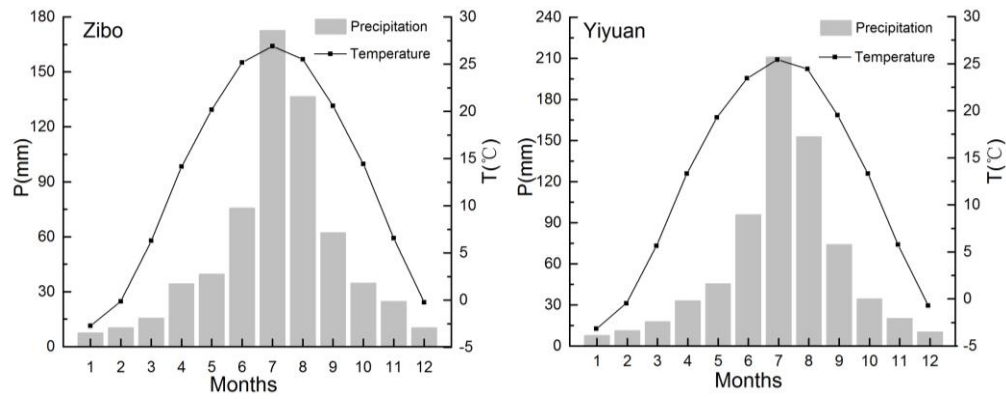
10 the Qinghai-Tibet Plateau. The green area is China, and the yellow area is the

11 other area.

12

1

2



3

4

5 Fig. 3. Monthly mean temperature (T) and precipitation (P) of Zibo (1952-1980) at  
6 Zibo Station and Yiyuan (1958-2005) at the Yiyuan Station, two meteorological  
7 stations close to the study site (Fig. 1).

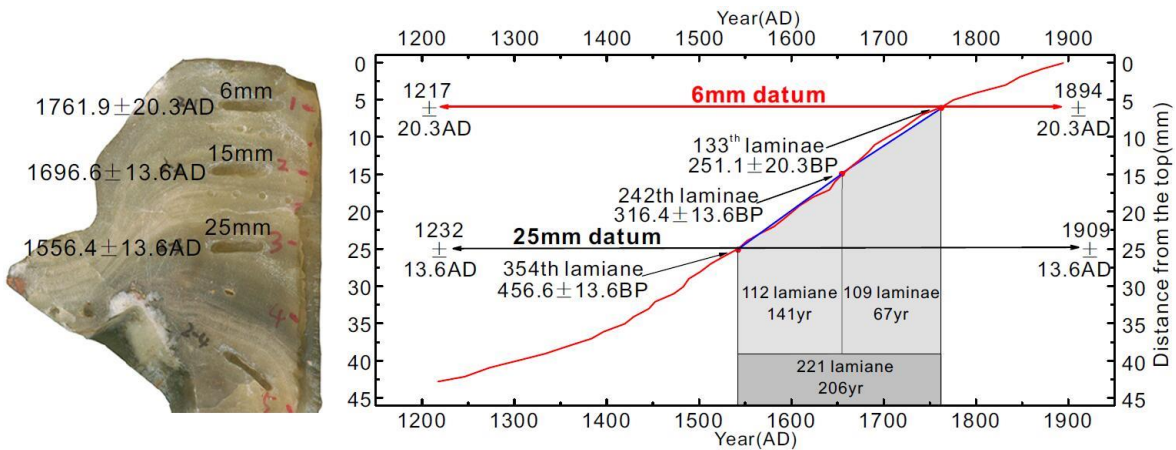
8



1  
2  
3  
4

Fig. 4. Polished longitudinal cross-section of stalagmite ky1

1

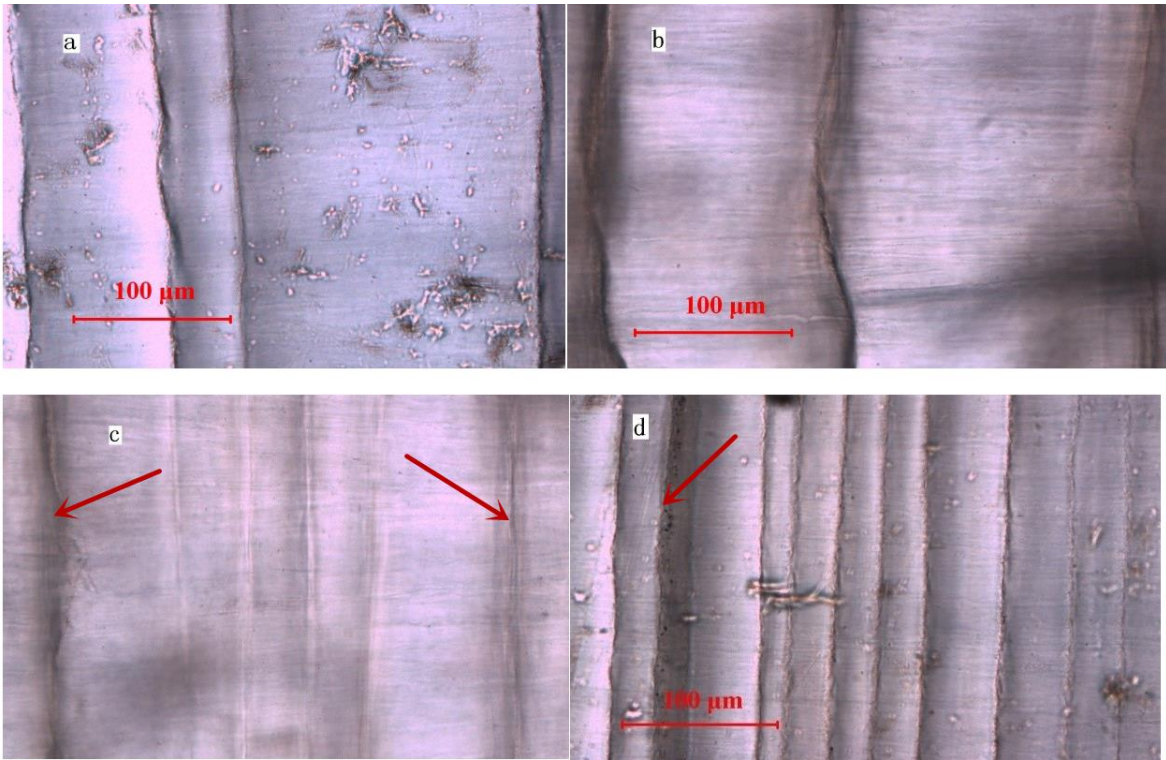


2

3 Fig. 5. The age model for stalagmite ky1 established by counting of laminae and  
 4 high precision dating results with the U-<sup>230</sup>Th technique. This figure is the photo of  
 5 stalagmite ky1, and the age label was based on high precision dating results with  
 6 the U-<sup>230</sup>Th technique on the left. The blue line is the high precision dating results  
 7 with the U-<sup>230</sup>Th technique and the connecting lines. The red line is the age scale  
 8 established by this article. The age of other laminae were determined by annual  
 9 laminae counting upward and downward based on the 133<sup>rd</sup> of the laminae  
 10 corresponding to the position of 6 mm, the age of which is 1762±20.3 AD decided  
 11 by high precision dating results with the U-<sup>230</sup>Th technique.

12

1



2

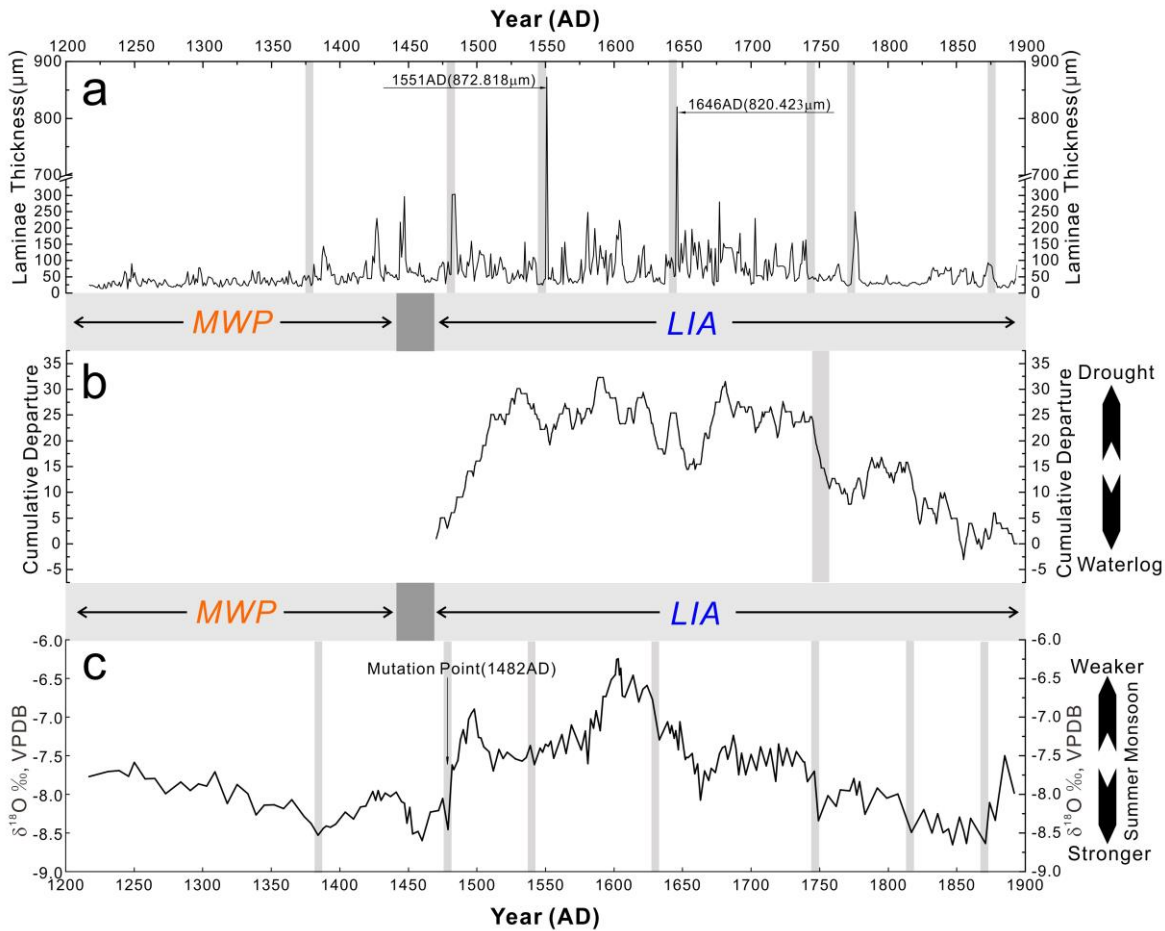
3

4 Fig. 6. The characteristics of the transmitting laminae in the upper part of  
5 stalagmite ky1 show that the thickness of the laminae has obvious variations. The  
6 boundary was curved, and the color near the boundary was deeper because of  
7 the dark transmitting laminae. The thickness of the laminae shows obvious  
8 variations (a), the curve of the boundary of transmitting laminae (b), the color  
9 variations of the boundary of transmitting laminae, the arrows indicating the  
10 darker boundaries, the boundaries in the middle were obviously whiter (c), dark  
11 transmitting laminae (d) (the arrows indicated in the figure).

12



1



2

3 Fig. 7. The year of formation and the thickness data series of the 678 laminae in the  
4 upper part (0-42.769 mm) of stalagmite ky1 (a), the cumulative departure curve (b)  
5 and the  $\delta^{18}\text{O}$  ratio data series for 172 samples (c). The thickness of the laminae  
6 formed in 1551 AD and 1646 AD were up to 872.818  $\mu\text{m}$  and 820.423  $\mu\text{m}$ ,  
7 respectively, much higher than other laminae. The cumulative departure curve (b)  
8 is drawn by drought/waterlog indices on the basis of the *Yearly Charts of*  
9 *Dryness/Wetness in China for the Last 500-Year Period (Chinese Academy of*  
10 *Meteorological Sciences of the China Meteorological Administration 1981)*, the  
11 curve has a rising trend representing less precipitation and the climate becoming  
12 drier, and the curve has a declining trend representing more precipitation and the  
13 climate becoming waterlogged.